ISTITUTO NAZIONALE DI RICERCA METROLOGICA
Repository Istituzionale

Intensity detection noise in pulsed vapor cell frequency standards

(Article begins on next page)

20 March 2024

Intensity detection noise in pulsed vapor cell frequency standards

Claudio E. Calosso, Michele Gozzelino, Aldo Godone, Haixiao Lin, Filippo Levi and Salvatore Micalizio

Laser intensity noise is currently recognized as one of the main factors limiting the short-term stability of vapor-cell clocks.

In this paper, we propose a signal theory approach to estimate the contribution of the laser intensity fluctuations to the short-term stability of vapor-cell clocks working in pulsed regime. Specifically, given a laser intensity noise spectrum, an analytical expression is derived to evaluate its impact onto the clock Allan deviation.

The theory turns out in good agreement with the experimental results obtained with a prototype of pulsed optically pumped (POP) Rb cell clock and can be extended to other compact clocks.

I. Introduction

Laser pumped vapor-cell clocks have recently achieved very good results in terms of frequency stability [1–6], reaching the 10^{-13} level for integration times τ of one second.
In the long term period, the best performances have been demonstrated operating the clock in pulsed regime. In this regard, two approaches have been successfully proved: the pulsed optical pumping (POP) and the pulsed coherent population trapping (CPT) techniques. In the first one, the atoms, after being optically pumped by a strong laser pulse, experience a couple of microwave pulses according to the Ramsey interrogation scheme. After that, a weak laser pulse is used to detect the atoms that have made the clock transition [7].

In the pulsed CPT, the atomic sample experiences a two-color laser pulse (Λ pulse) which prepares the atoms in the so called dark state. Then the atoms freely evolve for a time limited by the relaxation phenomena taking place inside the cell. Finally, a second Λ pulse probes the phase of the dark state. This scheme allows the detection of the so called Raman-Ramsey interference fringes [8–10].

In both approaches, the clock transition is commonly detected in the optical domain by monitoring the absorption profile of a probe laser after the passage through the cell. Laser amplitude noise is thus directly added to the error signal, degrading the clock performances via laser amplitude modulation to amplitude modulation (AM-AM) transfer [11].

Indeed, since other stability contributions (e.g. shot-noise and Dick-effect from the local oscillator) are kept in the low 10^{-14} [12], laser amplitude fluctuations, usually expressed in terms of relative intensity noise (RIN), may play an important role to limit the short-term stability of most of the state-of-the-art prototypes.

C. E. Calosso, A. Godone, F. Levi and S. Micalizio are with Istituto Nazionale di Ricerca Metrologica, INRIM, Torino, Italy.
E-mail: s.micalizio@inrim.it
M. Gozzelino is with INRIM and with Politecnico di Torino, Italy
H. Lin is with Key Laboratory of Quantum Optics, Shanghai Institute of Optics and Fine Mechanics, Chinese Academy of Sciences, Shanghai 201800 and with University of Chinese Academy of Sciences, Beijing 100049, China

Despite the importance of this topic, the laser detection noise has been considered in the literature only in few works [13,14] and often with ad hoc approximations. Some studies are reported in [15] and in [16] assuming since the beginning a white noise contribution to the clock final stability. This assumption is not always valid, especially in pulsed operation which involves clock cycle frequencies in the range 100 and 200 Hz (and relative multiples) where lasers have in general a flicker behavior.

Here we report a signal theory based approach leading to a more general evaluation of the laser RIN impact on the clock stability. Besides providing an analytical expression, the results of this work can be useful to impose precise constraints on the laser source needed to reach a given stability target.

The paper is organized as follows: in Section II we develop the theory, both in time and frequency domains. The proposed model aims to calculate the contribution to the stability $\sigma_y(\tau)$ for a clock in pulsed operation, given the laser relative intensity noise (RIN) expressed in terms of power spectral density. Specifically, two situations commonly found in the experiments will be discussed: laser RIN affected by white frequency noise and by flicker noise. Section III describes the experiments performed with a prototype of POP Rb clock. Conclusions are reported in Section IV.

II. Theory

We consider the experimental set-up depicted in Fig. 1 which can be adjusted to describe, for example, either a prototype of POP clock or a pulsed CPT clock. We are not interested to the details of the experimental apparatus (for example, in the case of pulsed CPT and electro-optic modulator, not shown in the figure, would be required).

The important issue in this context is that the laser signal at the input of the cell used to detect the clock transition is affected by intensity noise that will impact on the clock frequency. To evaluate this instability contribution, we take into account that the clock operation requires a sequence of steps, like construction of the error signal, sampling, etc.. well represented by input/output connections of functional blocks, typical of the signal theory [17]. The purpose of this section is then to provide the mathematical framework to describe how the optical detection signal is processed when a clock works in pulsed regime and how the laser intensity noise is transferred to the clock frequency.

A. Time domain analysis

With reference to Fig. 1, the laser intensity $I(t)$ impinging on the photodiode includes an average term I_0 and a random
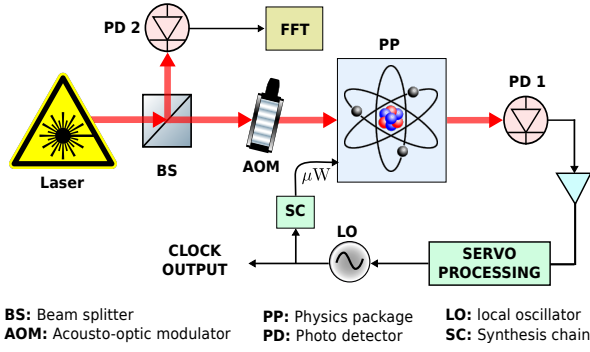
Figure 1. Proof of principle set-up schematic to study the impact of laser fluctuations on the clock frequency. PD1 is the photodiode used for clock purposes, PD2 is the photodiode used to characterize the intensity fluctuations of the free-running laser.

process $\delta I(t)$ with zero mean describing the noisy component of $I(t)$. It is convenient to introduce the relative intensity fluctuations defined as:

$$i(t) = \frac{\delta I(t)}{I_0} \qquad (1)$$

so that $I(t) = [1 + i(t)]I_0$.

Even if the clock works in pulsed operation, the laser signal (time domain) and the RIN spectrum (frequency domain, see later) are supposed to be acquired in continuous operation and before the cell. In this regard, the situation is similar to the Dick effect which provides an estimate of the clock frequency stability for a given free-running local oscillator noise. Moreover, we assume that the processes of pulsing and detecting are supposed ideal, therefore they do not add or alter the nature of the laser noise.

The clock operation commonly demands for the acquisition and the averaging of the signal over a detection window of duration τ_d; the averaging process acting on $i(t)$ is represented by the following impulse response:

$$h_a(t) = \begin{cases} \frac{1}{\tau_d} & \text{for } 0 \le t \le \tau_d \\ 0 & \text{elsewhere} \end{cases} \qquad (2)$$

We can define the fluctuations of the detected signal as $d(t) = h_a(t) * i(t)$, where $*$ stands for convolution product.

The laser detection pulse is used to read out the system status just after the interrogation phase (probe pulse); its intensity is then supposed low with respect to the pumping intensity and its duration τ_d much shorter than the relaxation times of the atomic sample.

The following step is the construction of an error signal $e(t)$ to feed the clock frequency loop. This is implemented by probing the left and right sides of the (even) atomic resonance. The error signal is computed as the difference between adjacent acquisitions of the signal taken at each cycle time T_c, where T_c includes pumping, interrogation, Ramsey and detection times. It is then the error signal itself which acts as frequency discriminator.

Its fluctuations can be evaluated as:

$$e(t) = d(t) - d(t - T_c) = h_\Delta(t) * d(t) \qquad (3)$$

As shown in Fig. 2, this step is represented by the block with the impulse response $h_\Delta = \delta(t) - \delta(t - T_c)$, where $\delta(t)$ stands for the Dirac delta function.

In pulsed regime, a signal sampling is present; it takes into account that the error signal is constructed every two basic clock cycles, that is every $2T_c$. This sampling process is formalized by $e_\delta(t)$, the sampled version of $e(t)$:

$$e_\delta(t) = e(t) \times 2T_c \sum_{k=-\infty}^{\infty} \delta(t - 2kT_c) \qquad (4)$$

where k is an integer, see Fig. 2.

The fluctuations of the sampled error signal are transferred to the local oscillator, supposed ideal, by the servo control loop through the discriminant of the error signal $D_e = 2\nu_0 D$, where ν_0 and D are the frequency and the slope of the atomic signal, respectively. In particular, for integration times $\tau > \tau_L$, being τ_L the time constant of the frequency loop we have:

$$y(t) = -\frac{1}{D_e} e_\delta(t) \qquad (5)$$

where $y(t)$ represents the fractional frequency fluctuations.

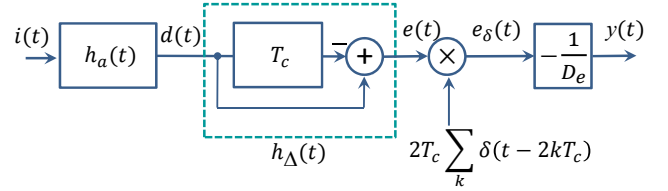All the aforementioned steps are summarized in Fig. 2.

Figure 2. Signal theory model of the laser detection processing for atomic clock purposes.

B. Fourier domain analysis

The time domain approach allowed us to define the main functional blocks and their interaction to describe how the optical detected signal is processed in a typical clock operation. The frequency domain analysis exploits the results of previous section to figure out how the RIN can affect the clock stability: RIN is indeed statistically specified in terms of its power spectral density (PSD) $S_i(f)$.

With reference to Fig. 2, we note that the first two functional blocks (acquisition over a detection window and construction of the error signal) are linear and time invariant. Thanks to a fundamental theorem of signal theory [18] we have:

$$S_e(f) = |H_a(f)H_\Delta(f)|^2 S_i(f) \qquad (6)$$

where $H_a(f)$ and $H_\Delta(f)$ are the Fourier transform of $h_a(t)$ and $h_\Delta(t)$, respectively, and $S_e(f)$ the PSD of the error signal. Specifically, $|H_a(f)|^2 = \text{sinc}^2(\pi f \tau_d) = \frac{\sin^2(\pi f \tau_d)}{(\pi f \tau_d)^2}$ and $|H_\Delta(f)|^2 = 4\sin^2(\pi f T_c)$

The next step is the sampling at $1/2T_c$ that induces aliasing since, in general, the bandwidth of $i(t)$ is much larger than the

sampling rate. High frequency noise in the range $\left[\frac{2k-1}{4T_c}, \frac{2k+1}{4T_c}\right]$ (where k is an integer) is folded back to base-band and adds up in power (quadratically), since any two frequency noise components are uncorrelated [19,20]. Therefore, we have:

$$S_{e_\delta}(f) = \sum_k |H_a(f_k)H_\Delta(f_k)|^2 S_i(f_k) \qquad (7)$$

where we defined $f_k \equiv f - \frac{k}{2T_c}$.

For clock purposes we are interested to assess how the laser RIN spectrum affects the clock stability, so our goal is to evaluate the clock Allan variance for averaging time $\tau \gg \tau_L$, or, in terms of spectrum, for low Fourier frequencies. In the limit $f \to 0$, it turns out $f_k \to \frac{k}{2T_c}$ and $H_\Delta(f_k) \to 0$ for k even and to 4 for k odd. This leads to:

$$S_{e_\delta}(f) \simeq \sum_{k \text{ odd}} 4 \left|H_a\left(\frac{k}{2T_c}\right)\right|^2 S_i\left(\frac{k}{2T_c}\right) \qquad (8)$$

that turns out a white noise, being independent on f.

The clock Allan variance is evaluated by scaling down the spectrum $S_{e_\delta}(f)$ by D_e^2 (see Eq. (5)). In addition, we take into account that the Allan variance for a given white noise level h_0 (bilateral) is $\sigma_y^2(\tau) = \frac{h_0}{\tau}$ [21], so we have:

$$\sigma_y^2(\tau) = \frac{4}{D_e^2} \sum_{k \text{ odd}} \text{sinc}^2\left(\pi \frac{k}{2T_c}\tau_d\right) S_i\left(\frac{k}{2T_c}\right)\frac{1}{\tau} \qquad (9)$$

Equation (9) holds for both bilateral and monolateral PSDs; obviously, the summation runs only on positive k in case of monolateral PSDs.
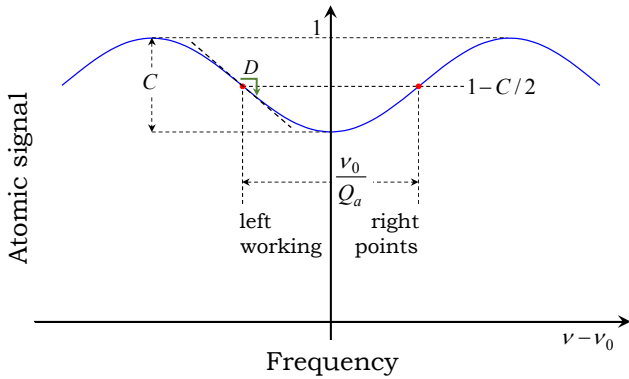

Figure 3. Ramsey fringes used to calculate the frequency discriminator D_e. The contrast C is defined with respect to the maximum of the clock signal; the clocks works at the signal level $1 - C/2$ when the left and right sides of the resonance are probed.

Equation (9) expresses how the laser intensity fluctuations during the detection phase affect the clock stability and is absolutely general; it applies to either the POP or the pulsed CPT standards. The specific technique adopted to detect the atomic resonance is defined by the term D_e. In particular, we consider the case where the clock transition is detected through the POP approach. With reference to Fig. 3, it is immediate to verify that:

$$D_e = \pi \frac{C}{1 - C/2} Q_a \qquad (10)$$

being C the contrast of the central Ramsey fringe, $Q_a = 2T\nu_0$ the atomic quality factor and T the Ramsey time.

1) Case of white frequency noise

It is interesting to apply Eq. (9) to the case of a laser whose RIN is mainly affected by white noise, $S_i(f) = h_0^i$. In this case, $H_a(f)$ acts as a low-pass filter with an equivalent bandwidth $B_e = \frac{1}{2\tau_d}$, so that the sum in Eq. (9) can be stopped to a certain k_e defined as the odd number closest to $\frac{B_e}{f_s} = \frac{T_c}{\tau_d}$, f_s being the sampling frequency $f_s = \frac{1}{2T_c}$:

$$\sigma_y^2(\tau) \simeq \frac{4}{D_e^2}\frac{k_e}{2}h_0^i\frac{1}{\tau} = \frac{2}{D_e^2}\frac{T_c}{\tau_d}h_0^i\frac{1}{\tau} \qquad (11)$$

Due to aliasing, the laser RIN is then degraded by a factor $2\frac{B_e}{f_s} = 2\frac{T_c}{\tau_d}$.

According to Eq. (11), the clock stability is apparently improved by increasing the detection time. However, an increase of τ_d leads to a reduction of the contrast C because the laser does not act anymore as a probe but can pump the atoms. Also, a reduction of T_c does not necessarily imply a better stability, since also the Ramsey time and then the Q_a are reduced accordingly. Indeed, the parameters in Eq. (11) are entangled and a wise and not trivial trade off among them is required in order to optimize the clock stability.

2) Case of flicker noise

It is as well of interest to consider a laser whose RIN is affected by flicker noise, $S_i(f) = h_{-1}^i/f$. In this case, considering that in many vapor cell clock arrangements $T_c \gg \tau_d$, we have that $\sum_{k \text{ odd}} \frac{2}{k}\text{sinc}^2\left(\pi\frac{k}{2}\frac{\tau_d}{T_c}\right) \simeq \ln\left(2\frac{T_c}{\tau_d}\right) + \gamma$, where γ is the Euler-Mascheroni constant. As a consequence, the Allan variance can be estimated as:

$$\sigma_y^2(\tau) \simeq \frac{2}{D_e^2}\left[\ln\left(\frac{T_c}{\tau_d}\right) + 0.878\right]2T_c h_{-1}^i\frac{1}{\tau} \qquad (12)$$

where $2T_c h_{-1}^i$ is the RIN level at the modulation frequency $\frac{1}{2T_c}$.

We observe that the stability scales logarithmically as the ratio T_c/τ_d only, therefore, in general it is not convenient to increase τ_d, also because of the consequent increase of T_c.

3) Case of spurs

Due to the aliasing phenomenon, spurs are a serious concern. In continuously operated clocks, spurs are generally considered out of frequency: a 50 Hz spur is about two orders of magnitude above the bandwidth of interest for calculating the Allan variance. Even a first-order low-pass filter provides an attenuation of 40 dB at 0.5 Hz.

In our case, instead, due to the sampling process inherent to the pulsed operation, the spur is directly converted to base band without any attenuation for frequencies below the equivalent bandwidth of H_a. The only viable solution is to tune the clock cycle T_c so that the spurs are as far as possible to the odd multiples of $\frac{1}{2T_c}$. Conversely spurs at even multiples are rejected by the digital lock-in. In this sense, the situation is different from the Dick effect, where odd multiples are rejected.

C. Sampling every clock cycle

A different locking protocol can be adopted. Specifically, we can apply the correction to the local oscillator every clock cycle T_c, by using every new clock acquisition together with the previous one, already available. In this way, together with the difference between the left and the right side of the resonance at $t = 2kT_c$, we have also the difference between the right and the left side for $t = (2k+1)T_c$, that has opposite sign. With respect to Eq. (4), this impacts on the sampled error signal, now available at time kT_c, as:

$$e_\delta(t) = e(t) \times T_c \sum_{k=-\infty}^{\infty} \cos\left(\pi \frac{t}{T_c}\right) \delta(t - kT_c) \qquad (13)$$

where it appears the additional demodulation factor $\cos\left(\pi \frac{t}{T_c}\right)$ that compensates for the change of sign between odd and even cycles.
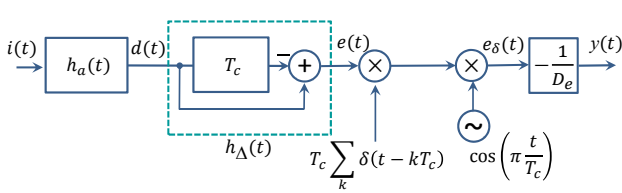
The equivalent block diagram is shown in Fig. 4.

Figure 4. Signal theory block scheme for sampling the clock signal every T_c.

The analysis in the Fourier domain now leads to

$$S_{e_\delta}(f) \simeq 2[1 + \cos(2\pi f T_c)] \sum_{k \text{ odd}} \left| H_a\left(\frac{k}{2T_c}\right) \right|^2 S_i\left(\frac{k}{2T_c}\right)$$
$$(14)$$

Since the degradation of the short-term stability is due to aliasing, we could expect an improvement when the sampling rate is doubled. In fact this is not the case, because (14) coincides to (8) for $f \to 0$. This protocol gives no significant advantages, at least for long averaging times ($\tau \gg 2T_c$).

III. EXPERIMENTS

The theory has been verified for the POP clock. The experimental setup is thoroughly described in [1]. Here we just recap the interrogation protocol and the experimental parameters which are of interest for the model validation.

The timing sequence is composed of an optical pumping pulse (0.4 ms), followed by a Ramsey sequence (3.8 ms) and finally an optical window is enabled to detect the clock transition (0.15 ms). The total cycle time, including short pauses between the different steps, is 4.39 ms. The pumping pulse power is 16 mW, whereas the detection probe power is $100 \, \mu\text{W}$. The Ramsey fringes obtained in this conditions show a contrast of 27.8% (see Fig. 3) and an atomic quality factor Q_a of 4.3×10^7. In clock operation, the correction on the LO frequency is performed every two cycles (i.e. every $8.78 \, \text{ms}$), thus following the protocol described in sections II A and II B.

In order to validate the model, the RIN has been artificially degraded by modulating the amplitude of the RF signal that drives the AOM. The amount of noise we injected is such that all other contributions to the short-term stability are completely negligible. In this particular condition, we can directly compare the measured clock stability to the stability predicted by the model given the measured laser intensity noise. We considered two common cases encountered experimentally: white and flicker noise. In Fig. 5 the noise levels, as measured before the clock cell, are shown. We measured a white noise level h_0^i of $1.7 \times 10^{-7} \, \text{Hz}^{-1}$ band-limited to $25 \, \text{kHz}$ and a flicker level h_{-1}^i of 4.8×10^{-6}, respectively. In Fig. 6 the
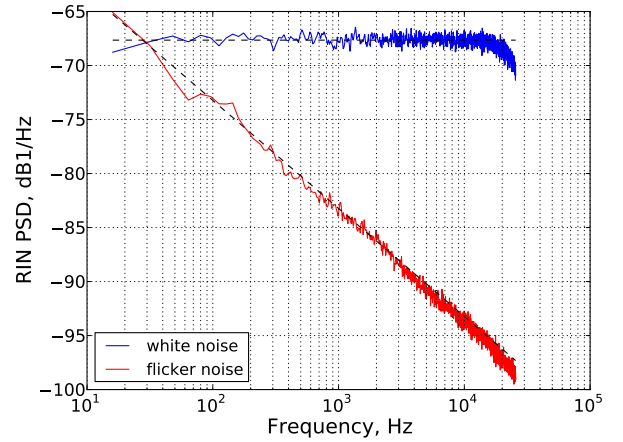

Figure 5. AM noise levels used in the model validation as measured at the input of the clock cell.

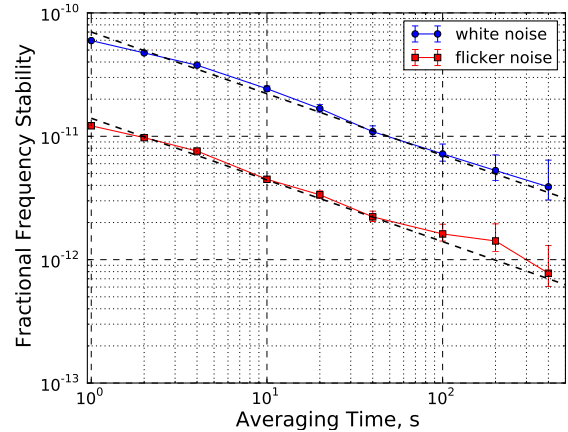measured clock stability for the two cases is shown.

Figure 6. Measured clock ADEV for the two cases considered in the text: laser RIN affected by white noise and by flicker noise.

In Table I we compare the measured stabilities to the results obtained with the model. Specifically, the Allan deviations for the two cases of white and flicker noises are estimated with Eq. (9) using as input the noise levels and the clock parameters (C, τ_d, T_c, T). In the two cases, also the approximate results of Eqs. (11) and (12) are reported. The results are consistent with the measured stability within 10%.

TABLE I
STABILITY MEASUREMENTS COMPARED TO THE ESTIMATE FROM THE MODEL

Input noise	Measured ADEV(1 s)	Estimated ADEV(1 s)	ADEV(1 s) from Eqs. (11) and (12)
White noise (1.7×10^{-7} Hz^{-1})	7.0×10^{-11}	6.4×10^{-11}	6.3×10^{-11}
Flicker noise ($4 \times 10^{-6}/f$)	1.4×10^{-11}	1.2×10^{-11}	1.2×10^{-11}

IV. CONCLUSION

In this paper we have analyzed how the laser intensity noise affects the short-term stability of a clock working in pulsed operation. Specifically, we developed a signal-theory model which accounts for all the operations required to lock the LO to the optically detected signal, including construction of the error signal and sampling. Given an arbitrary intensity noise spectrum of a free running laser, the model predicts the power spectral density of the clock error signal, and the corresponding contribution to the clock short term stability, once the shape of the resonance has been specified. In this regard, the paper results can be greatly useful in the clock design phase: for instance, by considering the laser RIN reported by the manufacturer and the expected clock signal parameters (contrast, quality factor, etc..), it is immediate through Eqs. (11) and (12) to give an estimate of the RIN contribution to the clock Allan deviation.

Also, the model gives more insight into the origin of the noise transfer, which is basically an aliasing process, as in the Dick-effect case. However, differently from the Dick effect, the Fourier frequencies of interest in the aliasing process are the odd multiples of $f_c/2$, due to the periodicity of the lock-in transfer function ($H_\Delta = 4\sin^2(\pi f T_c)$). This is in agreement with the intuitive reasoning that a sinusoidal noise does not interfere with the lock-in as long as its periodicity is equal to an even multiple of the lock-in differentiating cycle time ($2T_c$ corresponding to $f_c/2$).

The theory is absolutely general and can be easily extended to pulsed CPT vapor cell standards and also to other devices where the laser intensity noise is expected to play a role in affecting the frequency stability, like in compact cold atom clocks [22–24].

REFERENCES

[1] S. Micalizio, C. E. Calosso, A. Godone, and F. Levi, "Metrological characterization of the pulsed Rb clock with optical detection," *Metrologia*, vol. 49, no. 4, p. 425, 2012.

[2] S. Kang, M. Gharavipour, C. Affolderbach, F. Gruet, and G. Mileti, "Demonstration of a high-performance pulsed optically pumped Rb clock based on a compact magnetron-type microwave cavity," *Journal of Applied Physics*, vol. 117, no. 10, p. 104510, 2015.

[3] M. A. Hafiz and R. Boudot, "A coherent population trapping Cs vapor cell atomic clock based on push-pull optical pumping," *Journal of Applied Physics*, vol. 118, no. 12, p. 124903, 2015.

[4] G. Dong, J. Deng, J. Lin, S. Zhang, H. Lin, and Y. Wang, "Recent improvements on the pulsed optically pumped rubidium clock at SIOM," *Chin. Opt. Lett.*, vol. 15, p. 040201, Apr 2017.

[5] P. Yun, F. Tricot, C. E. Calosso, S. Micalizio, B. François, R. Boudot, S. Guérandel, and E. de Clercq, "High-performance coherent population trapping clock with polarization modulation," *Phys. Rev. Applied*, vol. 7, p. 014018, Jan 2017.

[6] T. Bandi, C. Affolderbach, C. Stefanucci, F. Merli, A. K. Skrivervik, and G. Mileti, "Compact high-performance continuous-wave double-resonance rubidium standard with $1.4 \times 10^{-13} \cdot \tau^{-1/2}$ stability," *IEEE Transactions on Ultrasonics, Ferroelectrics, and Frequency Control*, vol. 61, pp. 1769–1778, November 2014.

[7] S. Micalizio, A. Godone, C. Calosso, F. Levi, C. Affolderbach, and F. Gruet, "Pulsed optically pumped rubidium clock with high frequency-stability performance," *IEEE Transactions on Ultrasonics, Ferroelectrics, and Frequency Control*, vol. 59, pp. 457–462, March 2012.

[8] M. Abdel Hafiz, G. Coget, P. Yun, S. Gurandel, E. de Clercq, and R. Boudot, "A high-performance raman-ramsey cs vapor cell atomic clock," *Journal of Applied Physics*, vol. 121, no. 10, p. 104903, 2017.

[9] P. Yun, Y. Zhang, G. Liu, W. Deng, L. You, and S. Gu, "Multipulse ramsey-CPT interference fringes for the 87rb clock transition," *EPL (Europhysics Letters)*, vol. 97, p. 63004, mar 2012.

[10] R. Boudot, S. Guerandel, E. de Clercq, N. Dimarcq, and A. Clairon, "Current status of a pulsed cpt cs cell clock," *IEEE Transactions on Instrumentation and Measurement*, vol. 58, pp. 1217–1222, April 2009.

[11] J. Vanier and C. Mandache, "The passive optically pumped rb frequency standard: the laser approach," *Appl. Phys. B*, vol. 87, p. 565, 2007.

[12] B. Francois, C. E. Calosso, M. A. Hafiz, S. Micalizio, and R. Boudot, "Simple-design ultra-low phase noise microwave frequency synthesizers for high-performing Cs and Rb vapor-cell atomic clocks," *Review of Scientific Instruments*, vol. 86, no. 9, p. 094707, 2015.

[13] J. Danet, O. Kozlova, P. Yun, S. Guérandel, and E. de Clercq, "Compact atomic clock prototype based on coherent population trapping," *EPJ Web of Conferences*, vol. 77, p. 00017, 2014.

[14] S. Kang, M. Gharavipour, C. Affolderbach, and G. Mileti, "Stability limitations from optical detection in ramsey-type vapour-cell atomic clocks," *Electronics Letters*, vol. 51, no. 22, pp. 1767–1769, 2015.

[15] C. Audoin, G. Santarelli, A. Makdissi, and A. Clairon, "Properties of an oscillator slaved to a periodically interrogated atomic resonator," *IEEE Transactions on Ultrasonics, Ferroelectrics, and Frequency Control*, vol. 45, pp. 877–886, July 1998.

[16] G. Santarelli, P. Laurent, P. Lemonde, A. Clairon, A. G. Mann, S. Chang, A. N. Luiten, and C. Salomon, "Quantum projection noise in an atomic fountain: A high stability cesium frequency standard," *Phys. Rev. Lett.*, vol. 82, pp. 4619–4622, Jun 1999.

[17] L. L. Presti, D. Rovera, and A. De Marchi, "A simple analysis of the dick effect in terms of phase noise spectral densities," *IEEE transactions on ultrasonics, ferroelectrics, and frequency control*, vol. 45, no. 4, pp. 899–905, 1998.

[18] A. Papoulis, *Probability, Random Variables, and Stochastic Processes*. McGraw-Hill Book Company, Japan, 1965.

[19] F. Vernotte, G. Zalamansky, and E. Lantz, "Time stability characterization and spectral aliasing. Part II: a frequency-domain approach," *Metrologia*, vol. 35, no. 5, p. 731, 1998.

[20] J. W. Kirchner, "Aliasing in $1 f^\alpha$ noise spectra: Origins, consequences, and remedies," *Phys. Rev. E*, vol. 71, p. 066110, Jun 2005.

[21] C. E. Calosso, C. Clivati, and S. Micalizio, "Avoiding aliasing in allan variance: An application to fiber link data analysis," *IEEE Transactions on Ultrasonics, Ferroelectrics, and Frequency Control*, vol. 63, pp. 646–655, April 2016.

[22] F.-X. Esnault, D. Holleville, N. Rossetto, S. Guerandel, and N. Dimarcq, "High-stability compact atomic clock based on isotropic laser cooling," *Phys. Rev. A*, vol. 82, p. 033436, Sep 2010.

[23] F.-X. Esnault, E. Blanshan, E. N. Ivanov, R. E. Scholten, J. Kitching, and E. A. Donley, "Cold-atom double-Λ coherent population trapping clock," *Phys. Rev. A*, vol. 88, p. 042120, Oct 2013.

[24] P. Liu, Y. Meng, J. Wan, X. Wang, Y. Wang, L. Xiao, H. Cheng, and L. Liu, "Scheme for a compact cold-atom clock based on diffuse laser cooling in a cylindrical cavity," *Phys. Rev. A*, vol. 92, p. 062101, Dec 2015.